AADE-11-NTCE-23

Viscosity and Gel Structure: The Unseen Results of Their Manipulation

Jason Maxey, Halliburton

Copyright 2011, AADE

This paper was prepared for presentation at the 2011 AADE National Technical Conference and Exhibition held at the Hilton Houston North Hotel, Houston, Texas, April 12-14, 2011. This conference was sponsored by the American Association of Drilling Engineers. The information presented in this paper does not reflect any position, claim or endorsement made or implied by the American Association of Drilling Engineers, their officers or members. Questions concerning the content of this paper should be directed to the individual(s) listed as author(s) of this work.

Abstract

Drilling fluid design has long hinged on the balance between providing sufficient viscosity and gel structure to suspend solids (both cuttings and barite) and minimizing the rheological impacts on equivalent circulating density (ECD), pump initiation pressures, and swab and surge pressures. A wide variety of products and solutions are offered to boost or thin viscosity, boost "low-shear" viscosity, and control gel strength; all of these aim to provide suspension and hole cleaning with minimal ECD and risk from pressure spikes associated with initiating fluid flow. The *prima facie* supposition that increasing viscosity or yield point naturally leads to better solids suspension has been disproved through hard experience, while the idea that drillings fluids that appear significantly less rheologically "robust" can still provide suspension is now being observed. The exact reasons for these apparent contradictions are as yet poorly understood.

Currently, the rheological impact of various products and treatments are evaluated predominantly through the use of the standard FANN® Model 35 spring/bob viscometer. Both its ease of use and ubiquitous nature in the industry have led to a long reliance on this instrument as the best, most convenient source of rheological information on drilling fluids. Its shortcomings have been previously identified, and this paper endeavors to explore rheological differences through a variety of techniques on a lab-grade rheometer. Questions as to how and why various typical products affect viscosity and gel structure in invert emulsion fluids are explored, along with the implications to suspension and pressure spikes in drilling operations.

Introduction

The need for low viscosities for ease of flow in the annulus, the need for high viscosities to prevent fluid invasion and aid in hole cleaning, and the intermittent nature of the drilling process all compete for priority in the design of a successful drilling fluid. To meet these opposing criteria a mud must be a complex fluid, exhibiting viscoelastic properties to provide appropriate viscosities at the needed shear rates and also exhibiting viscoplastic properties through thixotropic and yielding properties to suspend solids in low-flow and stagnant conditions. For these reasons clays, which form associative networks or a microstructure in the fluid, are used as viscosifiers.

Traditionally, invert emulsion drilling fluids are prepared using various types of base oils emulsified with brine as the internal phase. Amine-treated bentonite (or other organophilic clay) is added, along with polymeric viscosifiers, to control rheological properties. Various lignitic and asphaltic materials may be added for filtration control, and barite or other weight material added to control density.[1-4] All of these components, including barite which is usually considered as inert in the system, interact to form the overall microstructure of the fluid. Any change in one of these components affects how everything interacts and thus affects the nature of the microstructure.

With modern options, the microstructure may be based around a traditional emulsion / organophilic clay interaction, or it may arise from emulsion only with no organophilic clays or solids added. These fundamentally different systems cannot be expected to behave the same way, and neither should the effect of various traditional oil-mud additives on microstructure (and thus rheology) be expected to be the same. It has long been observed that colloidal systems form associative microstructures based on several mechanisms, including:

- bridging,
- flocculation,
- steric stabilization,
- depletion attraction, and
- depletion stabilization.[5-7]

While these mechanisms are well known, they have been seldom applied to drilling muds beyond the thought that the bridging of emulsion droplets by organophilic clays as the main source of microstructure in traditional invert emulsion drilling fluids. This paper explores this concept through investigation of field muds with and without organophilic clays before and after treatment with various standard products.

Experimental Methods

Rheological testing was performed on an Anton-Paar MCR501 stress-controlled rheometer and compared to standard API measurements on a Model 35-type viscometer. In general, before testing, all fluids were brought to a test temperature of 120°F and then pre-sheared for two minutes immediately before beginning the test, significantly breaking the microstructure and providing a common starting point. When using a standard couette cell to produce a flow curve for

oil-based muds, wall slip significantly distorts measured data below ~1-s^{-1}. In order to avoid this problem, parallel plates which had been sandblasted to a 300-grit finish were used for testing. The slight roughness of the plates serves to greatly reduce the effects of wall slip and allows for relatively easy testing of fluids to rates as low as 10^{-4} s^{-1}. All tests were performed at a gap of 0.75-mm.

Many tests have been used over the years to evaluate the "strength" of the gel formed in muds and the yield stress.[3] The results of these tests often vary greatly, may or may not be correlated to one another for a given fluid, and ultimately may not lead to a significant understanding and differentiation of drillings fluids and their microstructure.

Treatment of a mud with various additives has long been recognized to affect, to a greater or lesser extent, the rheological properties of that fluid. A general understanding of the results of treatment has been made, but no real attempt to understand how these types of products influence microstructural growth (and thus broader rheological properties) has been undertaken. The focus of this paper is to begin to understand these microstructural influences through standard rheological techniques and through use of large amplitude oscillatory shear (LAOS) to examine yield stress and the energy required to break the microstructure in a single test.

LAOS

Several recent papers have examined drilling fluids through the LAOS technique.[4,8] The methodology followed here is similar to that previously reported by Maxey.[9] A good explanation of this method and the rheological parameters which can be obtained from it can be found in the recent papers by Ewoldt and McKinley[8,10] among other sources. In short it systematically connects, through a limited set of experiments, steady flow viscosity $\eta(\dot{\gamma})$, linear viscoelastic moduli G'(ω) and G"(ω), and nonlinear viscoelastic properties.[11] By examining the transient response of stress to an applied strain within the oscillation cycle, rather than by simply taking the absolute magnitudes of those oscillations, more information on the nature of the fluid can be obtained without disturbing the microstructure formed in the fluid.

For these tests, a triangular wave oscillation was applied at 0.1-rad/sec for strains of 10%, 50%, 100%, 500%, and 1000% (giving a maximum oscillation through ~180°). Triangular waves were used, rather than standard sinusoidal waves, for ease of set setup and data collection. As a result, the traditional moduli (G' and G'') do not have the same physical meanings and thus will not be discussed here. However, this test can be used to determine at what strains the fluid becomes fully yielded (where elastic and viscous contributions are overwhelmed by the plasticity of the fluid) while remaining in a closed-loop test where the fluid is stressed but not completely disturbed. By testing under fully yielded conditions, the following parameters can be obtained:

1. Yield Stress (τ_Y)
2. Peak, or overshoot, Stress (τ_P)
3. Energy Dissipation (E_D) in breaking microstructure

The typical response of a fluid to a triangular-wave LAOS at small and large strains is presented in Figure 1. At small applied strains, the stress response is roughly in the same form as the input – a triangular wave with some bending due to elasticity in the sample. For very large deformations the viscoelastic contributions are dwarfed by the yielding behavior and the stress response looks like a square wave.

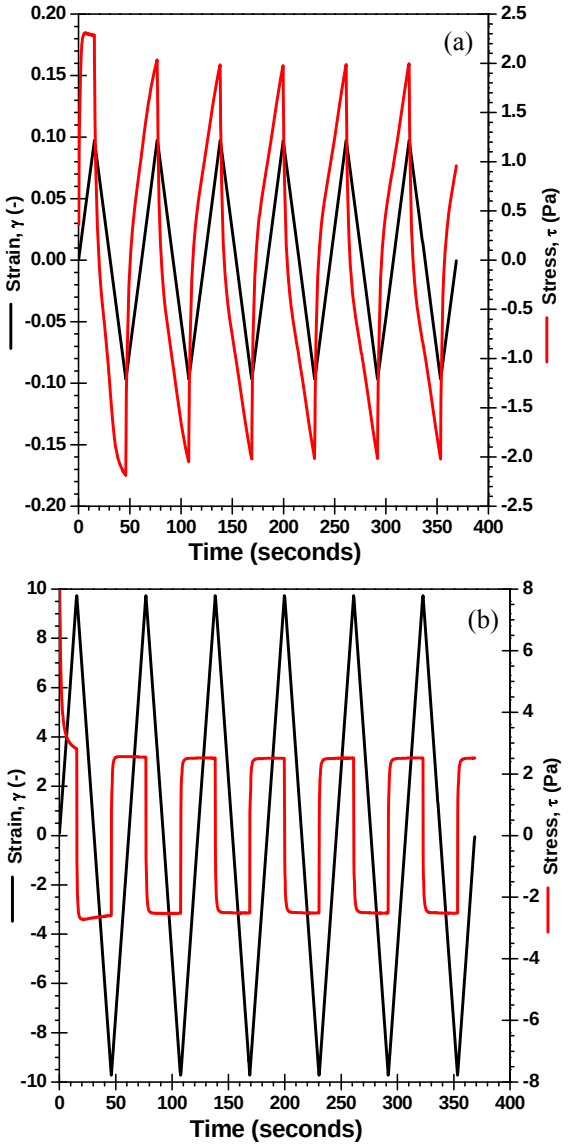

Figure 1 Triangular-wave LAOS raw data for a drilling fluid sample at (a) 10% and (b) 1000% strain amplitude.

A more convenient way to look at this data is using a Lissajous curve, plotting the stress as a function of strain. The data in Figure 1 is replotted in this way and presented in Figure 2a-2b. This allows one to view the test as an enclosed curve, which as an oscillatory test it is, and observe the transient response of stress as a function of strain. In this figure, each oscillatory cycle is presented as a different color curve. What is most obvious is that the first cycle is

appreciably different from subsequent cycles; this is the result of the start-up response of the mud to flow initiation. For the small strain case (Figure 2a) stress rises quickly in the first cycle and then plateaus before the flow direction reverses. This is due to partial yielding of the fluid at this strain, which becomes quickly dominated by viscoelastic response as the gel structure is partially broken and finds a steady state. Subsequent cycles do not display this yielding behavior, only the viscoelastic response of the fluid.

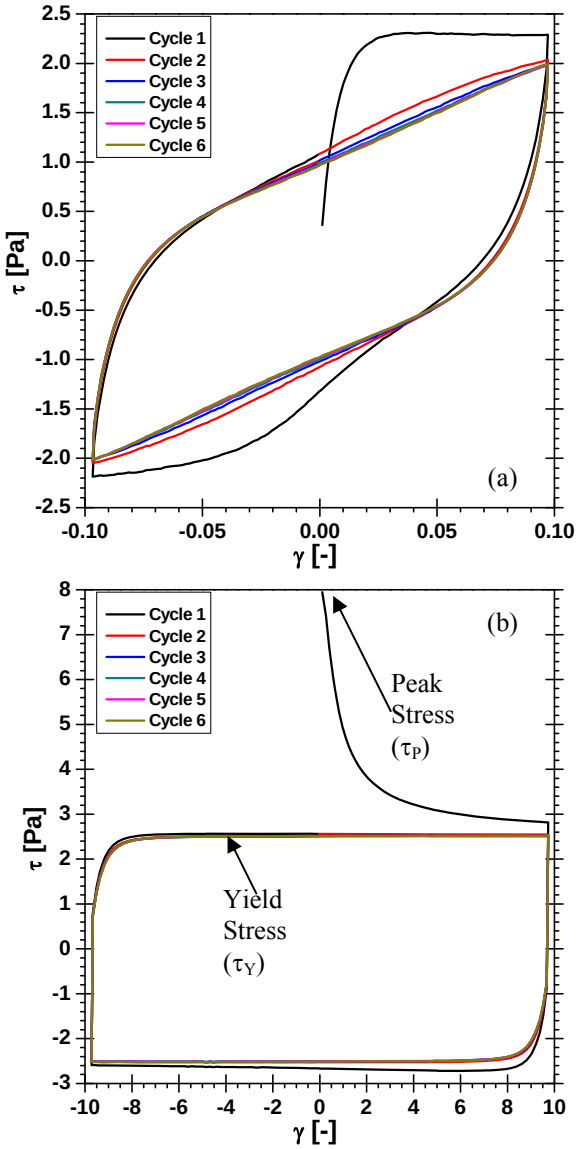

Figure 2 Raw data from Figure 1, for a drilling fluid sample at (a) 10% and (b) 1000% strain amplitude, replotted as Lissajous curves. A total of six oscillatory cycles are presented for each test.

The Lissajous curve for the 1000% strain test (Figure 2b) is quite different from the test at 10% strain. Rather than a slow rise to a plateau in the first cycle, a large spike is observed as a large stress (large amount of energy) is required to yield the fluid and initiate flow. Subsequent cycles are square, owing to the dominance of yielding, plastic behavior over viscoelastic responses at this strain, and approach a steady state with the microstructure broken. The magnitude of the peak stress, τ_P, varies from fluid to fluid, and is tracked in this paper as a parameter of interest. The stress plateau observed here does not change appreciably (at constant oscillatory frequency) once the fluid is fully yielded and is thus a reliable measure of the yield stress of the fluid. All data compared here is performed at 1000% strain amplitude, which was found to be fully yielded for all mud samples tested.

The stress required to initiate flow represents an energy burden for breaking microstructure in the fluid. The LAOS test is also ideal for examination of this energy. The energy for a single cycle can be found by simply integrating the stress as a function of strain

$$E_D = \int \tau d\gamma \qquad (1)$$

where E_D is the energy dissipation per unit volume. By evaluating E_D for each cycle individually, the energy required to initiate flow (cycle 1) can be compared to the energy required for flow at steady state (usually by cycle 6). This energy is that which is required to break microstructure in the fluid, is greatest in the first cycle (where most bonds are broken) and less in subsequent cycles as all microstructural bonds are broken over time. By comparing E_D in each cycle verses that at minimum value (usually steady state), and excess energy dissipation, E_D^E, is found

$$E_D^E = \sum_i \left(E_{D,i} - E_{D,min} \right) \qquad (2)$$

which shows the total energy per unit volume required to break microstructure and initiate flow at this strain. Here the methodology differs slightly from previous work, in that the excess energy dissipation is calculated at the minimum cycle energy dissipation rather than at long-time steady state. This is due to the observance that many fluids have a tendency to completely break gel microstructure after only a few cycles and then dynamically reform microstructure in subsequent cycles. The dynamic growth of structure in drilling fluids is well documented at low shear rates[3] and so only the point to where the structure is maximally broken (the dissipative energy minimum) is considered.

Test Fluids

For testing of the comparative effects of various common field mud additives, two invert emulsion drilling fluids were used as base fluids. One was a traditional OBM containing organophilic clays and other "black powder" products – OBM #1 – and the other was a high performance organophilic clay-free invert emulsion drilling fluid – OBM #2. These are the same fluids as Mud #6 and Mud #1, respectively, from previously published work.[9] These two fluids were selected because of their relatively similar basic properties (OWR, density, LGS) and because they form microstructure in fundamentally different ways. A relatively common type of product was added to a 1 lab barrel (350-ml) samples of each

mud and mixed on a multimixer for 30 minutes. The sample was then hot rolled at 150°F for 16 hours and re-sheared on the multimixer for 15 minutes before testing. Products added for testing included:

- lignite,
- polyamide polymer,
- carbon nanotubes,
- standard bentonite,
- dimer/trimer fatty acid (low-shear rheological modifier),
- organophilic clay (dry processed to amine treat),
- organophilic clay (wet processed to amine treat),
- fatty acid ether (an emulsifier),
- asphalt,
- fatty acid ester (low-shear rheological modifier),
- petroleum distillates (emulsifier),
- sepiolite, and
- 5-mm calcium carbonate.

Flow Curves

As a starting point to examine the effects of various common mud products on the rheology and microstructure of drilling fluids, flow curves on each fluid were measured at 120°F over shear rates of 10^{-4} s^{-1} to 1200 s^{-1}. The flow curves for the organophilic clay based mud are presented in Figure 3 and those for the organophilic clay-free mud are presented in Figure 4. To date, only half of the products tested on the organophilic clay-free mud have been tested on the organophilic clay-based mud. From this data it is observed

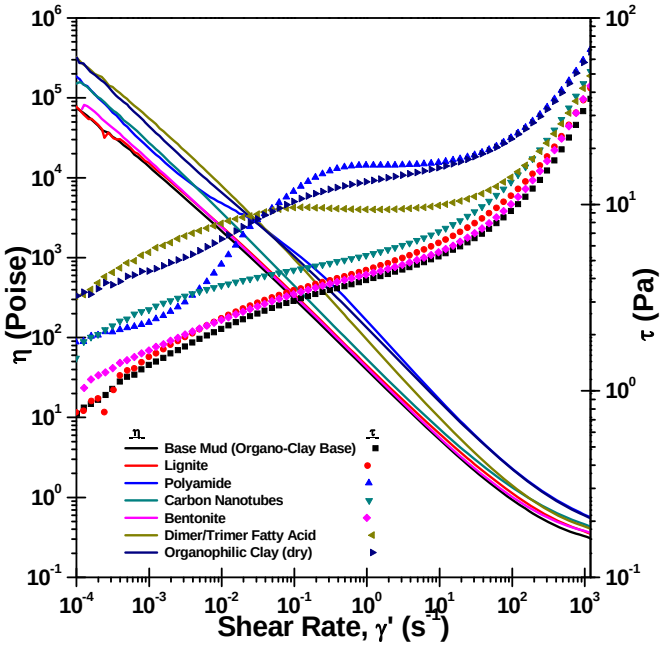

Figure 3 Flow curves at 120°F using sandblasted parallel plates for the organophilic clay-based invert emulsion mud, OBM #1, with various additives.

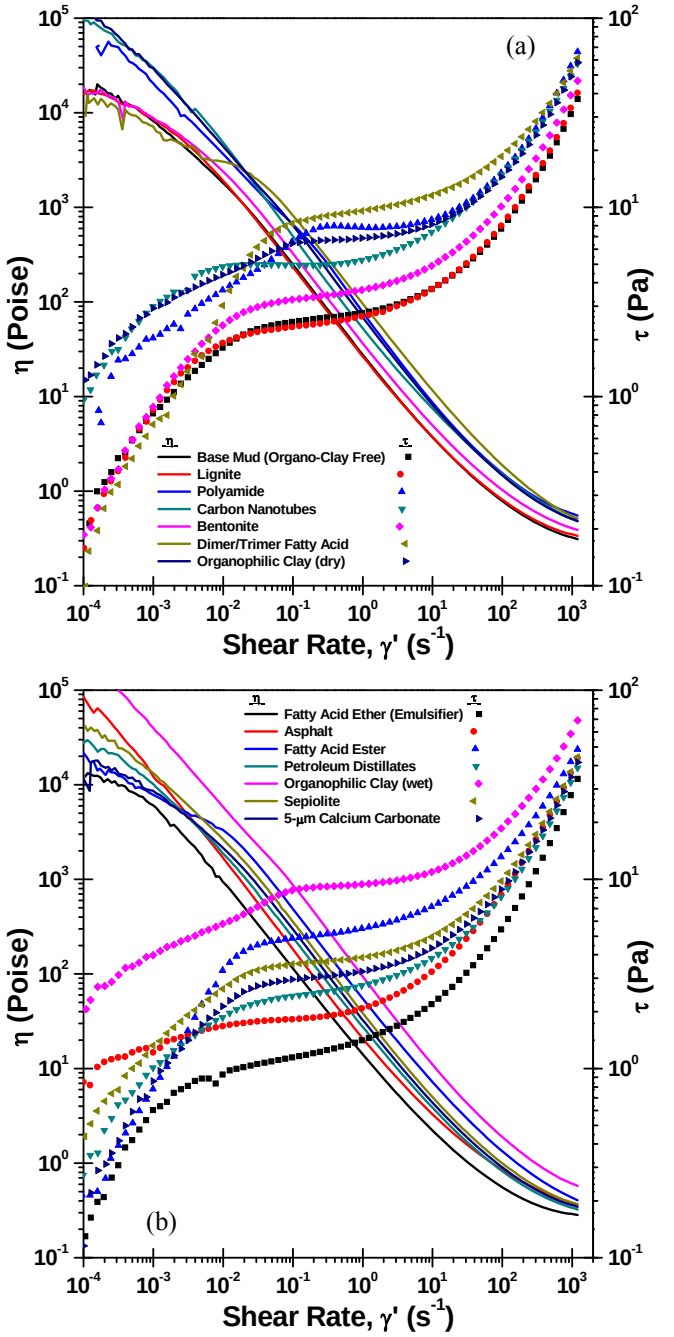

Figure 4 Flow curves at 120°F using sandblasted parallel plates for the organophilic clay-free invert emulsion mud, OBM #2, with various additives.

that while some products have a marginal effect on viscosity, others can greatly increase or reduce the viscosity. In addition, the magnitude of the change in viscosity is dependent on the differences in how the base fluid forms microstructure.

For example, the addition of carbon nanotubes has only a moderate effect on OBM #1, with the bulk of the effect being observed at very low shear rates. However, when added to OBM #2, the carbon nanotubes greatly increase the viscosity

and increased the observed yielding plateau by ~50%, from ~2.5 Pa to ~5 Pa. Similarly, the addition of dimmer/trimer fatty acid to OBM #2 significantly boosted viscosity at high and mid shear rates, but was identical to the base mud at very low shear rates. However, addition to OBM #1 resulted in minimal changes at high rates but a very large viscosity increase at low shear rates. Additions of organophilic clays, as expected, increased the viscosity in both muds as did addition of the polyamide polymer.

Aside from these general observations, and the fact that some additives have differing effects on the organophilic clay-based and clay-free fluids, no real information on how these products effect microstructural growth can be gleaned from just the flow curves. Further testing to examine the gel strengths of the fluids was thus performed.

Gel Tests

The gel strength of the various treated mud samples was tested using standard API procedures on a Model 35-type viscometer. In addition, a similar test was repeated on the MCR501 rheometer, where the sample was sheared, allowed to rest for 10-seconds, 10-minutes, or 30-minutes, and then a shear rate of 0.1 s^{-1} was applied (as opposed to the 5.11 s^{-1} rate applied in the API test) and the maximum overshoot recorded as the measured gel strength. When the 0.1 s^{-1} shear rate is applied, it is allowed to continue for a minimum of five minutes, usually long enough to achieve steady state. With this data, the energy required to break the gel structure and return to steady state can be calculated by integration of the stress as a function of strain (as done in the LAOS tests described above). The tests were performed on the rheometer in addition to the standard API test in order to address questions as to the validity of gel strengths measured by the API method. This is discussed in the following sections.

Validity of FANN Gel Measurements

Due to previous questions as to the validity of the gel strength as measured by standard API procedures, a simple test was devised and performed. In this test a coiled length of small diameter tubing is filled with a mud and immersed in a temperature bath held at 120°F. To one end of the coiled tubing is attached a reservoir of high-density brine which can be raised and lowered to increase the hydrostatic pressure applied to the mud in the coiled tubing. The reservoir is initially held so that the mud is static for a period of either 30 or 60 minutes, to allow full gel structure formation. At the end of the gel period, the reservoir is slowly raised until mud flow is observed at the exit of the coiled tubing. The hydrostatic pressure at this point is recorded at the pressure which break the gel structure and initiates flow. This pressure can then be related to the gel strength through momentum balance

$$\pi r^2 \Delta P = 2\pi r L \tau_w \qquad (3)$$

where L is the length of the tubing, r is the inner radius, ΔP is the pressure drop (equivalent to the measured hydrostatic pressure head), and with the assumption that the wall stress, τ_w, is the gel strength (that stress required to break the gel structure and initiate flow).

The length and diameter of the tubing used, as well as the API gel strengths and test results, are presented in Table 1. The calculated gel strength based on the measured pressure drop is found by Equation 3.

Table 1 Tubing and mud data from pressure to initiate flow in small tubing. All tests were conducted at 120°F.

	Tube #1	**Tube #2**
Actual Tube ID, in	0.22	0.343
Tube Length, ft	10	10
10-second API Gel Strength, lb/100 ft^2	7	7
10-minute API Gel Strength, lb/100 ft^2	15	15
30-minute API Gel Strength, lb/100 ft^2	18	18
Predicted Pressure to Break Gel, psi	2.73	1.75
Measured Pressure to Initiate Flow, psi		
Test 1 (30 minute gel)	1.07	0.76
Test 2 (30 minute gel)	0.97	0.66
Test 3 (30 minute gel)	1.02	0.71
Test 4 (60 minute gel)	0.97	0.86
Average ΔP, psi	1.00	0.75
ΔP per length of tube, psi/ft	0.1	0.075
Calculated gel strength, lb/100 ft^2	6.6	7.7

For both tests, in the 1/4" and 3/8" tubing, the gel strength calculated from experiments (after 30 minutes gel time) was close to the 10-second API gel strength, but less than half the 30-minute API gel strength. This result does seriously draw into question the validity of using the API gel strength measurement technique for calculation of downhole pressure drops when breaking gels and initiating flow, but is not unexpected. The nature of the flow initiation test – at a *relatively* high shear rate where viscoelastic effects are not negligible, while using a spring-bob torque sensor results in a measurement which is highly dependent on the spring and how fast the rotor reaches the set rotation speed, as well as superimposed shear effects with the gel breaking – all mix to make the API gel strength measurement machine-dependent and of questionable use. For this reason, gel strengths were measured on the MCR501 rheometer for this testing.

MCR501 Rheometer Gel Measurements

Gel strength tests as described above using the MCR501 rheometer are presented in Figure 5 for OBM #1 and in Figures 6 and **7** for OBM #2. A similar methodology for

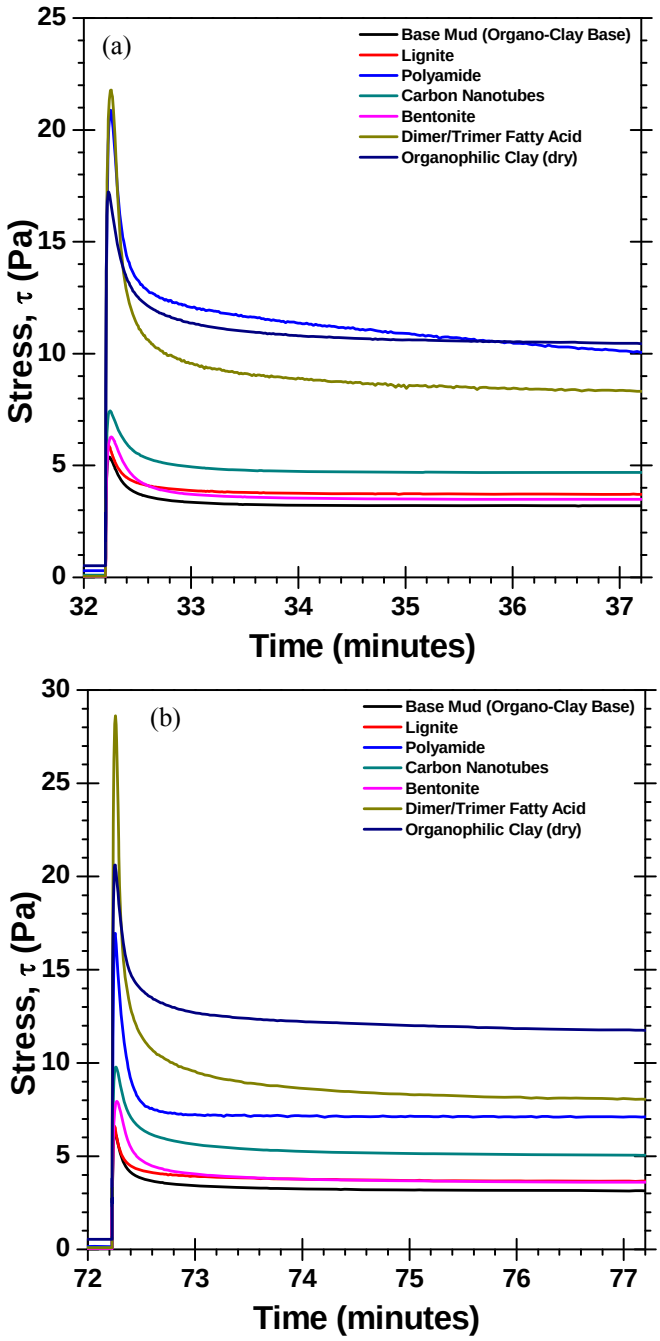

Figure 5 Gel strength measurements on the MCR501 rheometer for OBM #1 at 120°F after (a) a 10-minute gel period and (b) a 30-minute gel period.

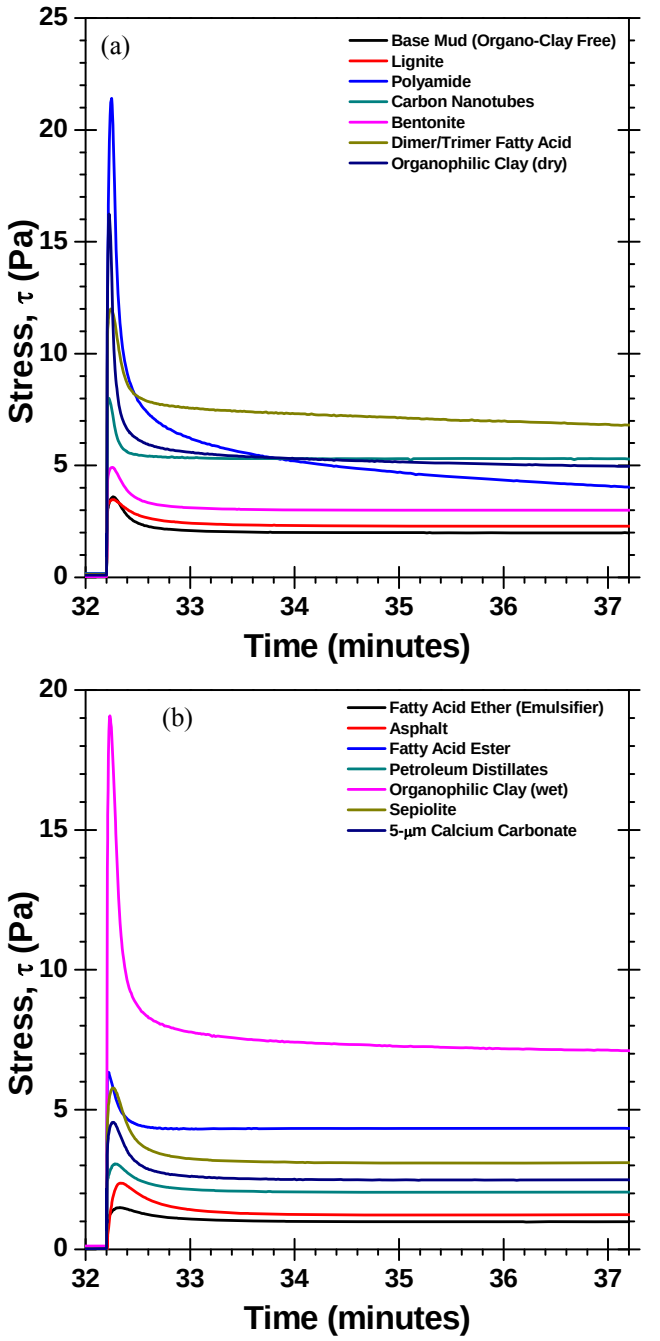

Figure 6 Gel strength measurements on the MCR501 rheometer for OBM #2 at 120°F after a 10-minute gel period.

testing at low shear rates applied to an instrument such as a Brookfield viscometer should give similar results. With these tests, some idea as to the effects of additives on microstructure begin to be seen. From the flow curves the viscosification effects were observed, but in the gel tests the differences in how these additives influence microstructure formation in fluids based on organophilic clays and those without organophilic clays is observed.

In gel tests on the MCR501 rheometer, after the gel period the shear rate was raised from 0-s^{1} to a stable 0.1-s^{-1} in ~0.01 seconds (fast transition, so minimal motor effects). The peak values were recorded and are presented, along with the API gel strengths, in Table 2 (for OBM #1) and Table 3 (for OBM #2). Contrasting effects of additives in the two mud systems can be observed in such additives as the dimmer/trimer fatty acid. In both muds, a large viscosification was observed when this was added; however, the increase in gel strength measured

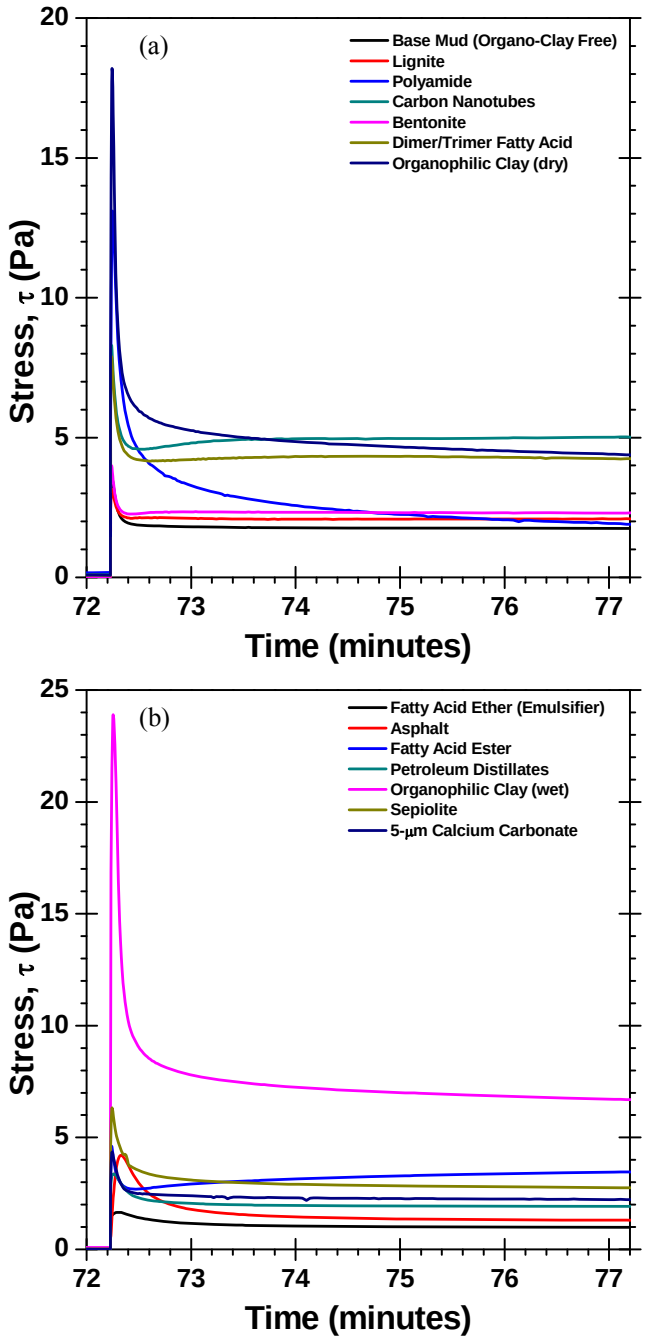

Figure 7 Gel strength measurements on the MCR501 rheometer for OBM #2 at 120°F after a 10-minute gel period.

by the MCR501 rheometer was much greater in OBM #1 than in OBM #2, indicating a synergistic effect with the growth of microstructure in the organophilic clay-based mud. The addition of carbon nanotubes, while not demonstrating a significant viscosification of OBM #1, results in slightly higher gel strengths than in OBM #2, again interacting differently with the dominant microstructures in both mud systems.

Addition of standard bentonite, while giving no significant viscosification of OBM #1 and showing modest viscosification to OBM #2, actually demonstrates a significantly larger increase in gel strengths in OBM #1. This result would, for example, tend to indicate that bentonite in an organophilic clay-free system produces a weak microstructure, such as would be expected from depletion attraction effects, while the more crowded system simultaneously results in increased viscosity. In an organophilic clay-based system,

Table 2 Gel strengths from API standard tests and gel tests on the MCR501 for OBM #1 at 120°F, after 10-minute and 30-minute gel periods.

	API Gels (lb/100 ft^2)		MCR501 Gel Tests (lb/100 ft^2)	
	10-min	30-min	10-min	30-min
Base Mud (Organo-Clay Base)	23	23	11.2	13.0
Lignite	24	24	12.4	13.8
Polyamide	54	56	43.6	35.4
Carbon Nanotubes	28	25	15.5	20.4
Bentonite	26	24	13.1	16.6
Dimer/Trimer Fatty Acid	35	29	45.5	59.8
Organophilic Clay (dry process)	39	32	36.0	43.1

Table 3 Gel strengths from API standard tests and gel tests on the MCR501 for OBM #2 at 120°F, after 10-minute and 30-minute gel periods.

	API Gels (lb/100 ft^2)		MCR501 Gel Tests (lb/100 ft^2)	
	10-min	30-min	10-min	30-min
Base Mud (Organo-Clay Free)	21	23	7.5	7.4
Lignite	21	23	7.3	6.6
Polyamide	54	56	44.7	27.4
Carbon Nanotubes	32	36	16.7	17.3
Bentonite	27	29	10.3	8.3
Dimer/Trimer Fatty Acid	44	45	25.1	16.5
Organophilic Clay (dry process)	42	45	33.9	38.0
Fatty Acid Ether (Emulsifier)	15	17	3.1	3.5
Asphalt	18	24	5.0	8.8
Fatty Acid Ester	30	32	13.2	9.6
Petroleum Distillates	20	20	6.4	7.1
Organophilic Clay (wet)	47	48	39.8	49.9
Sepiolite	30	32	12.1	13.2
5-µm Calcium Carbonate	27	28	9.5	9.1

however, stronger bonds are formed, possibly due to partial incorporation of the bentonite into the bridging structure of the existing amine-treated organophilic clays in the mud.

The above conclusions about the strength and type of effects bentonite have on the microstructures of the two mud systems are further demonstrated by observing the stress decline to steady state after the 30-minute gel peaks in Figure 5(b) and in Figure 7(a). The bentonite in OBM #2 falls rapidly to steady state, in less than 20 seconds. In OBM #1, however, ~2 minutes is required to reach steady state. This indicates a microstructure more resistant to disordering in OBM #1, such as would be expected from bridging of emulsion droplets. Similar differences are observed in the stress slope after the gel peak in the addition of polyamide polymer to the muds, where OBM #1 approaches steady state more rapidly than does OBM #2, and in the addition of dimmer/trimer fatty acid where the opposite effect is observed. A comparison of the energy dissipated in breaking the microstructure in gel tests on the MCR501 are presented in Table 4 for OBM #1 and Table 5 for OBM #2.

While this test is somewhat more beneficial than the standard API gel strength test, there are still some problems with it. For example, the gel strengths measured on the polyamide polymer addition decrease significantly from the 10-minute gel period to the 30-minute gel period. This is not likely due to a breakdown in microstructure in the mud over time, but is rather a sign of physical problems with the test (such as fluid fracture resulting in multiple flow regimes in the gap and only partial breakage of the microstructure). This would be less of a problem if using a vane stirrer rather than parallel plates for testing, but does demonstrate that in any test care must be taken to obtain good data and not junk data.

Triangular-Wave LAOS Results

LAOS experiments were performed on all mud samples using triangular-waves at a frequency of 0.1-rad/sec and multiple strains. Since all fluids exhibited fully developed yielding behavior at strain amplitudes of 1000%, data from these tests will be analyzed here. Some debate may be considered as to the proper strain at which to compare these fluids. One argument would suggest that using a uniform yielding strain for all comparative tests provides a simple basis to examine the energy dissipated in microstructure breakage with a minimal number of tests. This is the approach taken in this paper. Another argument would suggest the best comparison would be at the lowest strain at which each fluid fully yields, the yield strain. This has the advantage of potentially better portraying the actual energetic requirements for microstructure breakage when tripping pipe or during pump startup in drilling operations; however, this method requires many more tests and greater care to identify the yield strain. A third argument would promote the use of the gel point, the strain at which G' and G'' are equal, as a comparative point. This would not require an extensive test matrix, but would not reveal information on the actual yield stress or the overshoot experienced during flow initiation.

The energy dissipation, E_D, is plotted as a function of oscillatory cycle at 0.1-rad/sec, 1000% strain, and 120°F in Figure 8 (for OBM #1) and Figure 9 (for OBM #2). By observing the progress of E_D from peak in the first cycle to steady state we can draw conclusions as to the strength of microstructural bonds, and quantify this with the excess E_D value. This also further differentiates both the basic mud systems and how various additives affect their microstructures. While the base mud curves are relatively similar, with OBM #1 having a slightly higher E_D per cycle, the E_D^E for OBM #1 is significantly higher (see Tables 4 and 5). This indicates a stronger microstructural association in the organophilic clay-based mud – likely due to a bridging of emulsion droplets by the amine-treated clays – and a weaker microstructural association in the organophilic clay-free mud – likely indicating a predominately depletion attraction mechanism. These differences in microstructural mechanisms allow for design of muds which have similar flow properties and gel strengths but have lower energetic requirements for breaking gel structure and returning to steady flow conditions.

When the polyamide polymer is added to each mud, significantly different results are observed from results of flow curve and gel strength comparisons. From the viscometric and gel strength tests, there was little differentiation how the polyamide affects the two mud systems. Both resulted in fairly similar flow curves (both in form and magnitude) and the gel strengths measured by MCR501 were also very similar. In addition, τ_P for both mud systems with polyamide is nearly identical. However, the magnitude of E_D in each oscillatory cycle is significantly higher in OBM #1 (~650 J/m^3) than in OBM #2 (150-400 J/m^3), demonstrating a

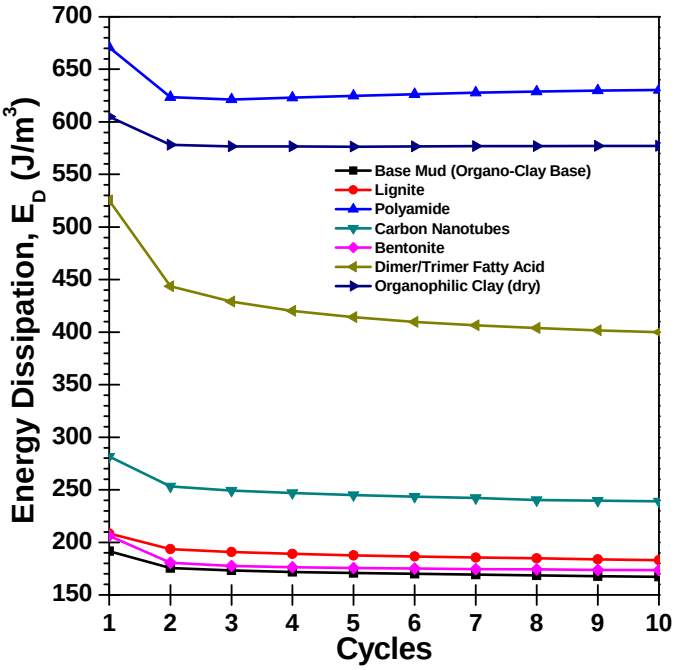

Figure 8 E_D from triangular-wave LAOS as a function of oscillation cycle for OBM #1 at 120°F at 0.1-rad/sec and 1000% strain.

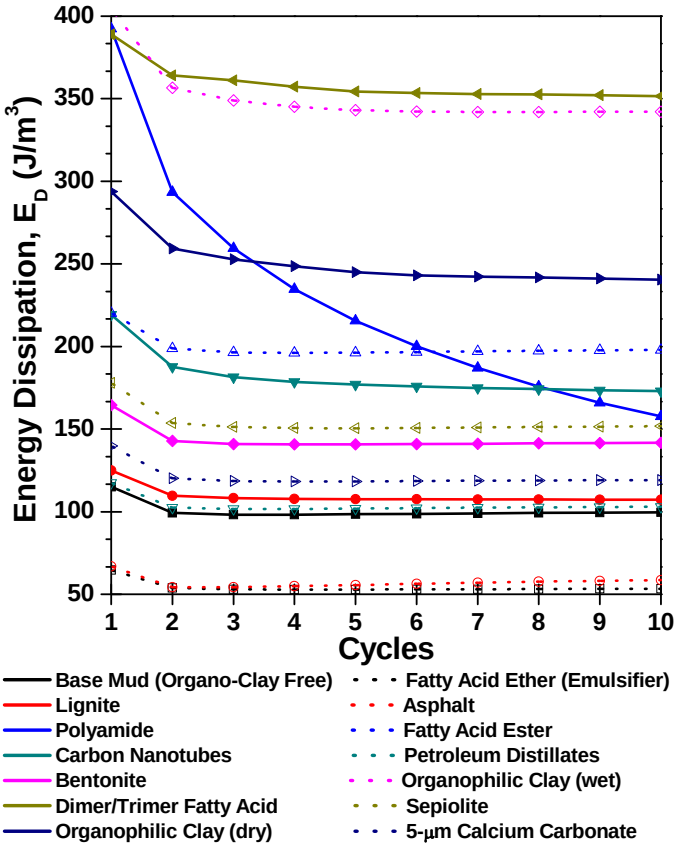

Figure 9 E_D from triangular-wave LAOS as a function of oscillation cycle for OBM #2 at 120°F at 0.1-rad/sec and 1000% strain.

stiffer response than previously indicated. However, in OBM #1 E_D rapidly reaches a minimum and returns to steady state, while for OBM #2 it continuously decreases through the 10 monitored cycles. As a result, the E_D^E in OMB #1 is ~7% of that for OBM #2. The energetic requirements to break the microstructure formed in OBM #2 with polyamide polymer strongly indicate that the polyamide bridges emulsion droplets, with a majority of the polymer involved in such connections. When added to OBM #1, however, the existing organophilic clays would appear to out-compete the polyamide polymer in creating emulsion droplet bridges, leaving the polymer to condense the microstructure through depletion attraction and only minimally change E_D^E.

Additions of organophilic clay (amine-treated through either a dry or wet process) have similar effects on the two mud systems. When added to OBM #2, the organophilic clays form bridging networks between emulsion droplets and the excess E_D increases ~500%. However, when more organophilic clays are added to OBM #1, the excess E_D actually decreases, possibly as a result of depletion stabilization of the emulsion droplet resulting in a less "sticky" microstructure. The value of τ_P for both systems is again very similar; however, τ_Y is significantly higher in OBM #1, despite a lower excess E_D.

Table 4 Peak stress, yield stress, and Excess E_D from triangular-wave LAOS OBM #1, compared with the energy dissipated in breaking microstructure in gel tests on the MCR501.

	LAOS			MCR501 Gel Tests (J/m^3)	
	τ_P (Pa)	τ_Y (Pa)	E_D^E (J/m^3)	10-min	30-min
Base Mud (Organo-Clay Base)	9.4	4.4	52.9	29.3	41.5
Lignite	9.2	4.8	62.0	29.7	39.9
Polyamide	33.3	16.8	51.6	124.0	141.0
Carbon Nanotubes	14.1	6.3	92.2	36.5	61.4
Bentonite	11.7	4.6	52.2	36.9	57.0
Dimer/Trimer Fatty Acid	41.2	10.3	255.4	176.7	282.9
Organophilic Clay (dry process)	25.8	15.1	30.4	85.2	115.7

Table 5 Peak stress, yield stress, and Excess E_D from triangular-wave LAOS OBM #2, compared with the energy dissipated in breaking microstructure in gel tests on the MCR501.

	LAOS			MCR501 Gel Tests (J/m^3)	
	τ_P (Pa)	τ_Y (Pa)	E_D^E (J/m^3)	10-min	30-min
Base Mud (Organo-Clay Base)	7.6	2.6	17.9	21.4	26.5
Lignite	6.5	2.8	23.2	15.2	16.1
Polyamide	33.1	4.1	704.4	220.7	145.1
Carbon Nanotubes	12.5	4.6	85.9	38.6	51.5
Bentonite	9.9	3.7	26.4	25.9	24.7
Dimer/Trimer Fatty Acid	24.7	9.2	73.9	62.4	52.9
Organophilic Clay (dry process)	25.4	6.2	103.3	155.5	191.3
Fatty Acid Ether (Emulsifier)	3.4	1.4	13.0	6.2	7.7
Asphalt	3.8	1.6	12.5	14.2	36.0
Fatty Acid Ester	12.4	5.2	27.2	28.9	25.0
Petroleum Distillates	6.0	2.7	16.6	13.2	19.4
Organophilic Clay (wet)	32.9	8.9	88.6	163.7	236.0
Sepiolite	11.9	4.0	31.4	36.1	47.3
5-µm Calcium Carbonate	8.8	3.1	23.9	27.9	29.0

The addition of two emulsifiers (the fatty acid ether and petroleum distillates) to OBM #2 demonstrates different results. For the addition of the petroleum distillates, minimum effect on the mud was observed, either in flow curves, gel strengths, or LAOS measurements. However, addition of the same amount of fatty acid ether emulsifier significantly decreased viscosity, decreased gel strengths by 50%, and decreased LAOS parameters. This could be due to the emulsifier causing a steric stabilization of the emulsion, reducing the connectivity of the microstructure and thus reducing rheological properties.

Finally, a comparison of the E_D^E from LAOS with the energy dissipated in gel strength tests on the MCR501 rheometer after 10-minute and 30-minute gel periods can be made in Tables 4 and 5. In many cases, the excess energy dissipation calculated from LAOS is significantly different, usually higher, than that observed from gel strength testing. This could be a result of differences in oscillatory and rotational testing. In a rotational test, the fluid is constantly sheared in a single direction. When testing yielding fluids using parallel plates, some degree of shear banding or flow fracture is possible in the gap, the measured stress response will be different and thus the calculated energy to reach steady state will not include complete breakdown of the gel structure. In an oscillatory test, however, shear banding is less likely to occur and the full breakdown of the gel structure will be observed and measured in the test. The use of a vane stirrer would likely bring the two measurements into better agreement.

Conclusions

- Differences in microstructural mechanisms allow for design of muds with similar flow properties and gel strengths but lower energetic requirements for breaking gel structure and returning to steady flow conditions.
- The addition of various common oil mud additives can affect the way in which microstructure forms in the invert emulsion fluid. Standard rheological techniques can give a superficial view of these effects, and combined with LAOS can give insight as to microstructural growth mechanisms.
- Understanding of mechanisms for microstructure formation in invert emulsion fluids allows for better planning of how the mud will behave downhole, including under pump initiation, tripping pipe, drill ahead and shut-in situations. This understanding may also lead to better understanding of the mechanisms of barite sag.
- Fluids designed to build microstructure without the benefit of organophilic clays or other strong natural emulsifiers exhibit significant disruption in performance when such materials are added to the system.
- Standard oilfield rheological testing methods are insufficient to determine potential mechanisms for microstructural formation. The API standard gel strength measurement, while useful, is known and demonstrated to be highly inaccurate and cannot provide reliable data to monitor more subtle changes in gels.

Acknowledgments

The author would like to thank Halliburton for granting permission to publish the paper.

Nomenclature

LAOS = *Large Amplitude Oscillatory Shear*
G' = *Storage modulus (Pa)*
G'' = *Loss modulus (Pa)*
τ = *Stress (Pa)*
τ_Y = *Yield Stress (Pa)*
τ_P = *Peak Stress (Pa)*
τ_w = *Wall Stress (Pa)*
η = *Viscosity (Poise)*
E_D = *Energy dissipation per cycle per unit volume (J/m^3)*
E_D^E = *Excess E_D (J/m^3)*

References

1. Herzhaft, B., et al. Influence of Temperature and Clays/Emulsion Microstructure on Oil-Based Mud Low Shear Rate Rheology, *SPE Journal*, 211-217 (2003).
2. Gandelma, R.A., et al. Study on Gelation and Freezing Phenomena of Synthetic Drilling Fluids in Ultradeepwater Environments, SPE/IADC 105881, 2007 SPE/IADC Drilling Conference.
3. Maxey, J. Thixotropy and Yield Stress Behavior in Drilling Fluids, AADE-07-NTCE-37, AADE 2007 National Technical Conference.
4. Maxey, J., R. Ewoldt, P. Winter, and G. McKinley. Yield Stress: What is the "True" Value?, AADE-08-DF-HO-27, AADE 2008 Fluids Conference.
5. Araki, T. and H. Tanakaasd. Dynamic depletion attraction between colloids suspended in a phase-separating binary liquid mixture, *J. Phys.: Condens. Matter* **20**(7), (2008).
6. Otsubo, Y. Rheology Control of Suspensions by Soluble Polymers, *Langmuir*, **11**(6), 1893-1898 (1995).
7. Pickrahn, K., B. Rajaram, and A. Mohraz. Relationship between Microstructure, Dynamics, and Rheology in Polymer-Bridging Colloidal Gels, *Langmuir*, **26**(4), 2392-2400 (2010).
8. Ewoldt, R., P. Winter, J. Maxey, and G. McKinley. Large amplitude oscillatory shear of pseudoplastic and elastoviscoplastic materials, *Rheologica Acta*, Online First preprint.
9. Maxey, J. A Rheological Approach to Differentiating Muds by Gel Structure, AADE-10-DF-HO-27, AADE 2010 Fluids Conference.
10. Ewoldt, R. H., A. E. Hosoi and G. H. McKinley. New measures for characterizing nonlinear viscoelasticity in large amplitude oscillatory shear, *Journal of Rheology* **52**(6), 1427-1458 (2008).
11. Dealy, J. M. and K. F. Wissbrun. *Melt rheology and its role in plastics processing : theory and applications*. (Van Nostrand Reinhold, New York, 1990).